

## Numerical analysis of rectangular rafts on layered foundations

R. A. FRASER\* and L. J. WARDLE\*

The behaviour of perfectly smooth, uniformly loaded rectangular rafts of any rigidity resting on a homogeneous elastic layer which is underlain by a rough rigid base is analysed. Graphical solutions are presented which enable the determination of vertical displacement at the centre, mid-edges and corner of the raft, and the maximum bending moment in the raft. The solutions have been obtained by the finite element method with the interaction between raft and finite soil layer being incorporated through the use of surface elements. A weighting method is presented which allows an approximate isotropic modulus to be derived for a multi-layered soil permitting the solutions to be applied to multi-layered foundations. Variations in raft rigidity and length/breadth ratio and soil layer depth and Poisson's ratio can markedly effect both displacements and bending moments in raft foundations.

On analyse le comportement de radiers rectangulaires parfaitement lisses, chargés uniformément, de n'importe quelle rigidité, reposant sur une couche élastique homogène située au-dessus d'une base rugueuse, rigide. Des solutions graphiques sont présentées qui permettent la détermination du déplacement vertical au centre, au milieu des bords et aux coins du radier, et du moment de flexion maximum dans le radier. Les solutions ont été obtenues par la méthode des éléments finis, l'interaction entre radier et la couche de sol d'épaisseur finie étant prise en compte en utilisant des éléments de surface. Une méthode de pesantier est présentée, qui permet d'obtenir un module isotrope approximatif pour un sol à couches multiples permettant aux solutions d'être appliquées aux fondations sur couches multiples. Les variations de la rigidité des radiers, du rapport longueur/largeur, de la profondeur de la couche du sol et du coefficient de Poisson peuvent affecter d'une façon marquée aussi bien les déplacements que les moments de flexion dans les radiers.

The designer of rectangular raft foundations has very little information readily available for the estimation of both total and differential settlements and maximum bending moments in the preliminary design phase. Computer programs, e.g. FOCALS (Wardle and Fraser, 1975) are now available which will consider superstructure/raft/soil interaction, but these require the input of raft thickness from a preliminary design for the final detailed design.

A crude estimate of maximum differential settlement across a raft and total settlement of the raft can be made using available solutions for uniformly loaded rectangular areas on finite elastic layers.

At one extreme full flexibility can be assumed. In this case Ueshita and Meyerhof (1968) and Milovic and Tournier (1971) have presented information on the displacement at the corner of a uniform rectangular load on an elastic layer of finite thickness overlying a rough rigid base. Thus central and differential settlements can be conservatively estimated. At the other extreme of a rigid raft, Giroud (1972) proposed that the average settlement over a uniformly loaded rectangular area on an elastic layer represented the settlement of a rigid rectangular load, and presented appropriate tables of average settlements. However, this technique gives no information about raft thickness for detailed design of a raft of intermediate flexibility.

## NOTATION

$t$	raft thickness	$R$	bending moment correction factor for finite layer thickness
$b$	raft breadth	$n$	number of plate finite elements
$l$	raft length ( $l \geq b$ )	$E_{h, v}$	cross-anisotropic elastic moduli (eqns 9)
$K$	raft stiffness factor	$\nu_{hv, vh, h}$	cross-anisotropic Poisson's ratios (eqns 9)
$d$	soil layer depth	$f$	cross-anisotropic shear modulus (eqns 9)
$\nu_r$	Poisson's ratio of raft	$\epsilon_{x, y, z}$	direct strain components
$\nu_s$	Poisson's ratio of soil	$\gamma_{xy, xz, yz}$	shear strain components
$E_r$	modulus of elasticity of raft	$\sigma_{x, y, z}$	direct stress components
$E_s$	modulus of elasticity of soil	$\tau_{xy, xz, yz}$	shear stress components
$E^*$	$= E/(1 - \nu^2)$	$a_{11, 33, 13}$	cross-anisotropic elastic constants (eqns 12)
$p$	applied uniform load	$\alpha$	cross-anisotropic elastic constant (eqns 12)
$\rho$	settlement		
$I$	settlement influence factor		
$S$	settlement correction factor for finite layer thickness		
$m$	bending moment per unit width		
$M$	bending moment influence factor		

For rigid raft foundations on a semi-infinite elastic soil layer there are solutions available for contact stress, bending moment and shear force. Gorbunov-Possadov and Serebrjanyi (1961) have presented solutions for contact pressure and bending moment for a square slab subject to a central concentrated load. Butterfield and Banerjee (1971) have given solutions for settlement and contact pressure for rigid rectangular rafts. Brown (1972) obtained solutions for contact pressure and bending moment in rigid, square and rectangular rafts subject to various combinations of concentrated loads. Chan and Cheung (1974) have given values of contact pressure for rectangular and circular rigid footings due to concentric and eccentric loading. These solutions enable an estimate to be made of the bending moment in a rigid footing.

In this Paper, numerical solutions are presented for the displacements and maximum bending moments for uniformly loaded raft foundations of arbitrary flexibility on a homogeneous isotropic elastic layer of finite thickness overlying a rough rigid base. The Appendix shows how the results for the isotropic semi-infinite medium can be applied to a cross-anisotropic semi-infinite medium.

Details of how the graphical solutions presented can provide approximate solutions for multi-layered media are also given.

## METHOD

The first satisfactory solutions for square rafts of arbitrary flexibility were obtained by Cheung and Zienkiewicz (1965). The stiffness of the soil was derived from the Boussinesq equation and combined with plate bending finite elements to form a stiffness matrix for the whole system. The displacements were solved using the finite element method. Cheung and Nag (1968) used a similar technique to allow for horizontal contact pressures beneath the raft, and for uplift between the plate and soil. Svec and Gladwell (1973) improved the method of Cheung and Zienkiewicz by assuming a continuous contact pressure distribution, described by a third degree polynomial, under each plate finite element. They also developed a 10-node triangular plate bending element specifically for contact problems.

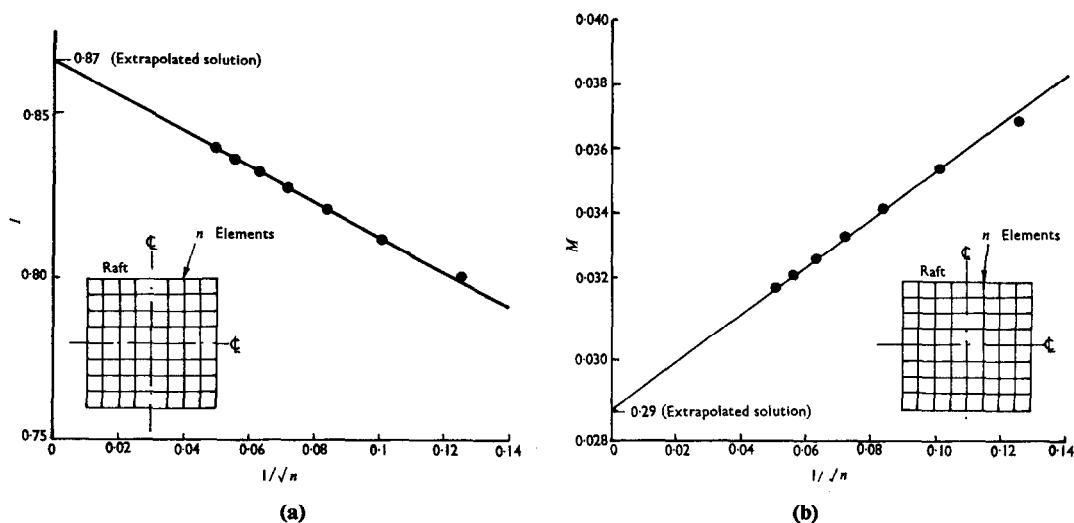


Fig. 1. Convergence of solutions for rigid square raft: (a) settlement; (b) maximum bending moment

Wardle and Fraser (1974) extended the approach of Cheung and Zienkiewicz to a multi-layered soil system, investigating the effects of a finite homogeneous soil layer and a soil modulus that increased linearly with depth. The results presented in this Paper have been derived using the computer program FOCALS (Wardle and Fraser, 1975). The computer program performs a static elastic analysis of rafts of arbitrary rigidity and variable thickness resting on a layered soil mass. The response of the loaded area of the soil system is modelled using surface elements (Wardle and Fraser, 1975). The surface element stiffness matrix is derived from the surface settlements due to uniformly loaded rectangular areas, obtained using integral transform techniques (Gerrard and Harrison, 1971). The layered soil mass consists of any number of horizontal layers of uniform thickness, with infinite lateral extent. The bottom layer may rest on a rigid base or extend to infinite depth.

The surface element approach offers many advantages over conventional three-dimensional finite elements. Only the portion of the surface of the soil mass that is loaded needs to be discretized; for conventional finite elements the whole volume of soil needs to be discretized, leading to many degrees of freedom and the imposition of artificial boundary conditions. A comparison between both methods applied to a square raft on a finite layer indicated that the degrees of freedom and band width modelled using surface elements were much smaller than for brick elements and the total solution time was smaller by a factor of 20 (Wardle and Fraser, 1974).

The raft (and any superstructure) is modelled using conventional finite elements. The computer program can also consider rafts that are not rectangular in plan or which contain cut-outs. In addition, cross-anisotropic soil properties can be used. Consideration of anisotropy is particularly important for overconsolidated soils where the deformation moduli in the vertical and horizontal directions are different and the independent shear modulus is lower than expected from isotropic theory (Gerrard *et al.*, 1972).

For simplicity of analysis the contact between the raft and the soil is assumed to be frictionless. Hooper (1974) indicated that the presence of an adhesive interface between the raft and the soil can significantly reduce differential raft displacements. For a uniformly loaded

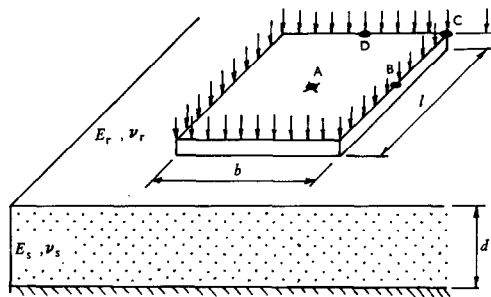


Fig. 2. Rectangular raft on homogeneous layer

fully flexible circular raft resting on a semi-infinite soil mass with Poisson's ratio,  $\nu_s$ , equal to 0, central settlement is reduced by 16% and differential settlement by 44% when full adhesion is considered. For a completely rigid circular raft full adhesion leads to a 9% reduction in settlement for  $\nu_s = 0$ . When  $\nu_s = 0.5$ , no lateral surface displacements occur under the raft and the adhesive and frictionless cases give identical results. Hooper (1975) demonstrated similar behaviour for a cross-anisotropic half-space. In practice, interfacial slip will limit the extent of these reductions.

#### ACCURACY OF ANALYSIS

The accuracy of the solutions was found to depend markedly on the degree of discretization used. The effect which varying the number of plate elements has on the convergence of the displacements and bending moments is illustrated in Fig. 1, for a rigid square raft on a semi-infinite soil mass. The results for a range of meshes are plotted against  $n^{-1/2}$ , where  $n$  is the number of plate elements for the whole raft. (Only one quarter of the raft was used in the computer analysis.) For  $n > 36$ , the results fall on a straight line. The correct solution is assumed to be given by extrapolation of the straight line to the limit  $n^{-1/2} = 0$ . All of the problems examined in this Paper exhibited similar behaviour. To maximize the accuracy of the solutions, this extrapolation technique has been used throughout.

Confirmation of the likely accuracy of the extrapolated solutions is given by comparison with other published solutions for the settlement of a uniformly loaded square rigid raft on a semi-infinite soil mass. The extrapolated solution obtained from Fig. 1 is  $I = 0.87$ . By comparison, Gorbunov-Possadov and Serebrjanyi (1961) give  $I = 0.88$  and Absi (1970) gives  $I = 0.87$ .

#### INFLUENCE CHARTS

Graphical solutions for the settlements and bending moments in a uniformly loaded rectangular raft are presented in this section. The supporting soil system consists of a homogeneous isotropic layer of thickness  $d$  resting on a rigid base (Fig. 2).

The stiffness factor for the system is defined by:

$$K = \frac{4 E_r (1 - \nu_s^2) t^3}{3 E_s (1 - \nu_r^2) b^3} \quad \dots \dots \dots (1)$$

where  $E_r$  is the modulus of elasticity of the raft,  $\nu_r$  is the raft Poisson's ratio,  $E_s$  is the modulus of elasticity of the soil,  $\nu_s$  is the soil Poisson's ratio,  $t$  is the raft thickness and  $b$  is the raft width.



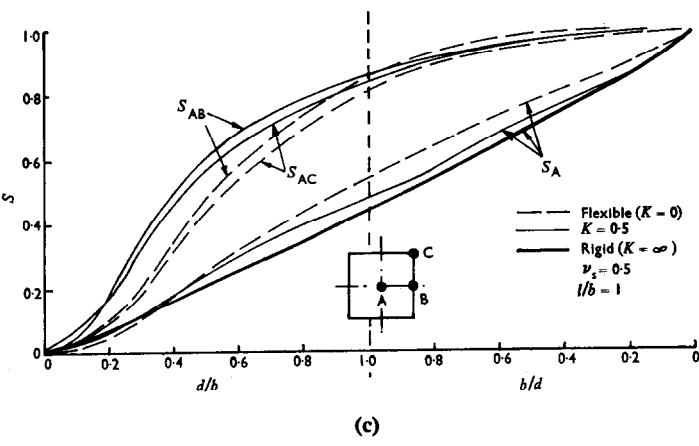
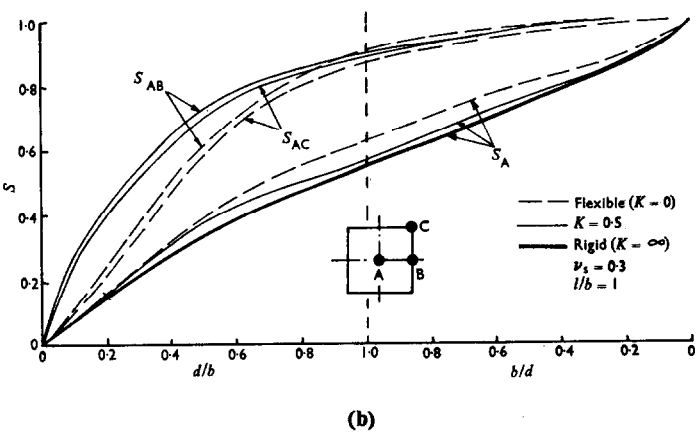
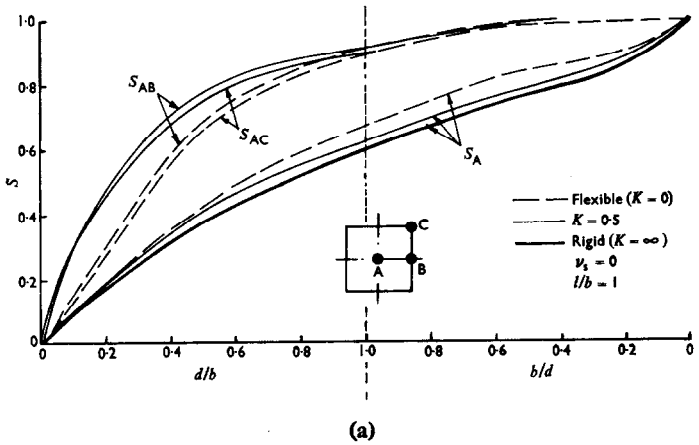


Fig. 4. Settlement correction factor  $S(l/b=1)$ : (a)  $\nu_s=0$ ; (b)  $\nu_s=0.3$ ; (c)  $\nu_s=0.5$

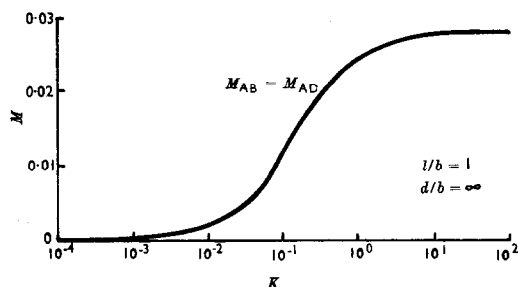


Fig. 5. Bending moment influence factor  $M$  for  $d/b = \infty$ , ( $l/b = 1$ )

#### Charts for $l/b = 1$

Values of settlement influence factor  $I$  are given in Fig. 3 and correction factors,  $S$ , for finite layer depth in Fig. 4. The corresponding bending moment influence factor  $M$  and correction factors,  $R$ , are given in Figs 5 and 6.

The effects on the finite layer depth are clearly demonstrated by Figs 4 and 6. For a layer thickness equal to the raft width, predictions of total settlement differ by as much as 55%, differential settlement by 18% and maximum bending moment by 15% when compared with a semi-infinite soil mass. In general, the effect of finite layer depth becomes greater as Poisson's ratio approaches 0.5. The relative stiffness factor  $K$  of the raft-soil system is a major factor in determining its performance. Note that from eqn (1), with other factors kept constant,  $K$  is proportional to the ratio of the raft modulus to the soil modulus. Therefore while a raft founded on rock may behave flexibly, the same raft founded on soft clay would behave rigidly.

From Figs 3 and 5 it can be seen that the most rapid change in performance is the range  $0.05 < K < 0.5$ .

A system with  $K$  less than 0.01 can be considered fully flexible. That is, decreasing the raft thickness below the value associated with  $K$  equal to 0.01 produces only a very small difference in the overall performance of the system. Similarly, a system with  $K$  greater than unity can be considered fully rigid, and increasing raft thickness will have little effect on performance.

#### Charts for $l/b = 2$

The influence charts for  $l/b = 2$  (Figs 7–10) are similar to those for  $l/b = 1$  (Figs 3–6). Again the most rapid change in performance is in the range  $0.05 < K < 0.5$ , and the effect of finite layer depth becomes greatest as Poisson's ratio approaches 0.5.

The effect of finite layer thickness is greater than for the case  $l/b = 1$ . Considering the effect of a finite layer of thickness  $b$  beneath such a raft, it is found that central settlement can be decreased by 63%, differential displacement by 50% and bending moment by 20% in the short direction and by 45% in the long direction from the values for a semi-infinite soil mass.

#### Charts for $3 < l/b < 5$

In situations where the  $l/b$  value exceeds 2 and consequently falls outside the range of the influence charts in Figs 3 to 10, the charts in Figs 11–16 can be used to provide an estimate of settlement, differential settlement and bending moment.

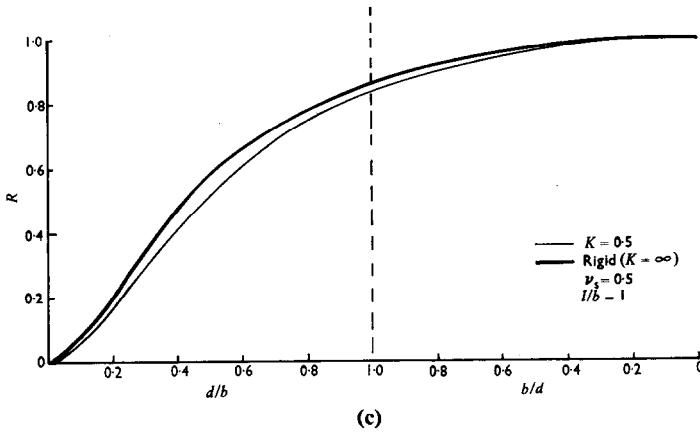
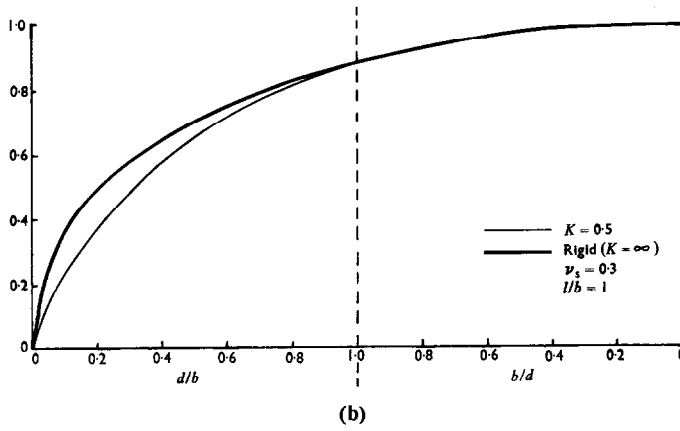
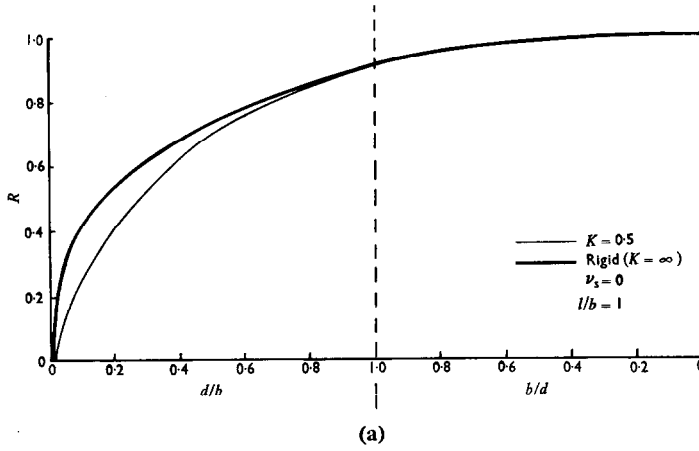


Fig. 6. Bending moment correction factor  $R(l/b=1)$ : (a)  $\nu_s=0$ ; (b)  $\nu_s=0.3$ ; (c)  $\nu_s=0.5$



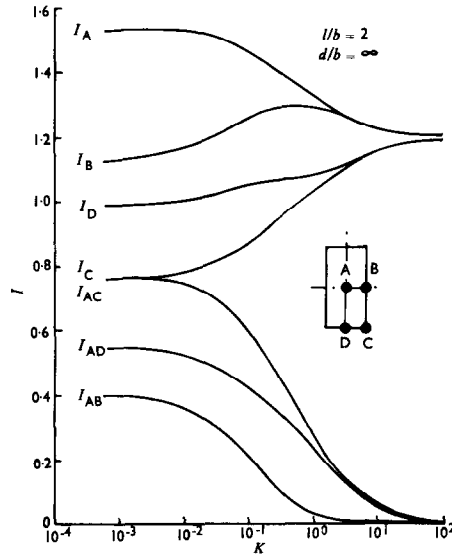


Fig. 7. Settlement influence factor  $I$  for  $d/b = \infty$ , ( $l/b = 2$ )

Figure 11 gives influence coefficients for central displacement for  $l/b$  values in the range 1 to 5 for a semi-infinite medium ( $d/b = \infty$ ) and Fig. 12 gives similar curves for  $d/b = 1$ . Although the actual curves for  $3 < l/b < 5$  do not actually coincide, the line drawn is accurate to within  $\pm 5\%$ . Figs 13 and 14 give similar influence coefficients for differential displacement. Fig. 14 provides values of  $I_{AB}$ ,  $I_{AC}$ ,  $I_{AD}$  directly for  $3 \leq l/b \leq 5$ . The curves for these values of  $l/b$  do not coincide exactly but are accurate within  $\pm 5\%$ . Figs 15 and 16 provide values of maximum bending moment  $M$  for  $d/b$  equal to infinity and 1 respectively. In Fig. 16 values for  $\nu_s = 0.3$  only are given. For  $K$  values ranging from flexible to  $K = 1$  they are accurate for all positive values of Poisson's ratio to within  $\pm 10\%$  and for  $1 \leq K \leq 10$  to within  $\pm 30\%$ . For  $\nu_s = 0$  the value indicated increases, and for  $\nu_s = 0.5$  it decreases.

For values of  $d/b$  not equal to 1 or  $\infty$ , the influence coefficients can be obtained by interpolation. Charts similar to those in Figs 4, 6, 8 and 10 should be constructed by drawing a smooth curve of similar shape through the influence coefficient points for  $d/b = 0, 1$  and  $\infty$ .

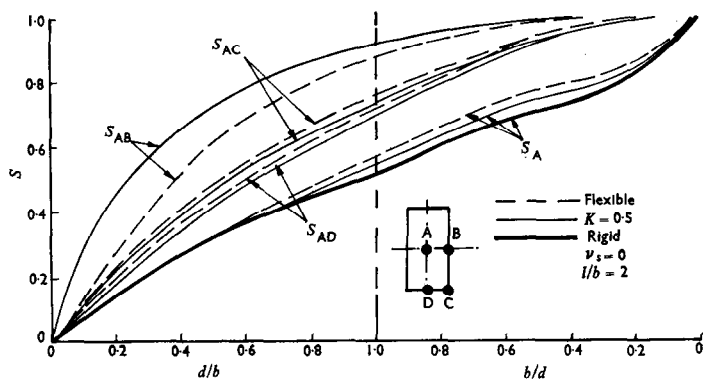
## NUMERICAL EXAMPLE

Consider a square raft foundation of dimensions 10 m by 10 m and 0.5 m thick, subject to a uniform load of 0.1 MPa resting on a soil layer of thickness  $d = 40$  m. The raft Young's modulus,  $E_r$ , is 15 000 MPa and Poisson's ratio  $\nu_r = 0.2$ , and for the soil the values are  $E_s = 83.2$  MPa and  $\nu_s = 0.3$ . Using  $E_r = 15$  000 MPa,  $\nu_r = 0.2$ ,  $t = 0.5$  m,  $b = 10.0$  m,  $E_s = 81.9$  MPa,  $\nu_s = 0.3$ , eqn (1) gives  $K = 0.0289$ .

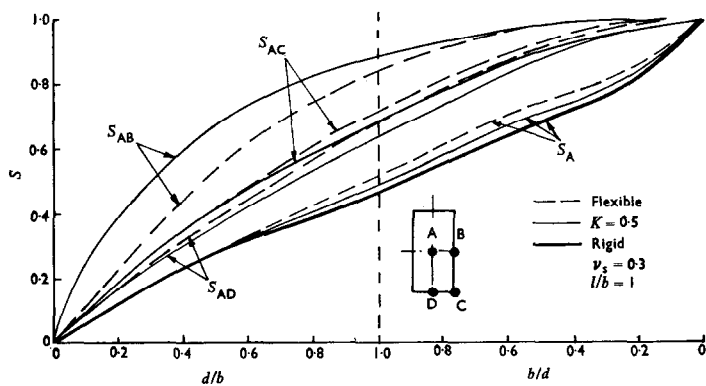
### Central settlement

For a semi-infinite soil mass, Fig. 3 gives  $I_A^{sl} = 1.10$ . Eqn (2) then gives:

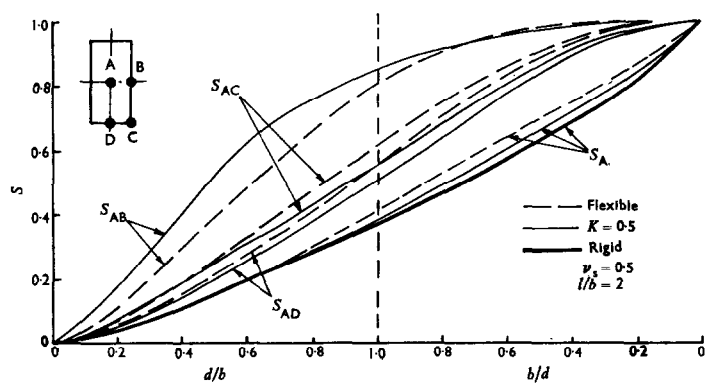
$$\rho_A^{sl} = pb \frac{(1 - \nu_s^2)}{E_s} I_A^{sl}$$



(a)



(b)



(c)

Fig. 8. Settlement correction factor  $S(l/b=2)$ : (a)  $\nu_s=0$ ; (b)  $\nu_s=0.3$ ; (c)  $\nu_s=0.5$

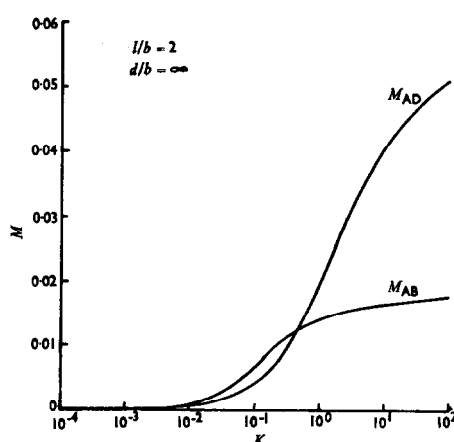


Fig. 9. Bending moment influence factor  $M$  for  $d/b = \infty$ , ( $l/b = 2$ )

$$= \frac{0.1 \times 10.0 \times 0.91 \times 1.10}{81.9}$$

$$= 0.0122 \text{ m}$$

The correction factor  $S$  for the effect of the finite layer depth is obtained from Fig. 4(b). Since  $K = 0.0289$  represents a very flexible raft,  $S_A = 0.88$  for  $d/b = 4.0$ . Eqn (4) then gives:

$$\rho_A = S_A \rho_A^{sl}$$

$$= 0.88 \times 0.0122$$

$$= 0.0107 \text{ m}$$

### Differential settlement

From Fig. 3,  $I_{AB} = 0.26$ , giving  $\rho_{AB}^{sl} = 0.0029$ . Multiplying by the correction factor,  $S_{AB} = 1.00$  gives:

$$\rho_{AB} = 0.0029 \text{ m}$$

### Maximum bending moment

For a semi-infinite soil mass, Fig. 5 gives  $M^{sl} = 0.005$ , and from eqn (3)

$$m^{sl} = 0.1 \times 10.0 \times 10.0 \times 0.005$$

$$= 0.05 \text{ MN m/m}$$

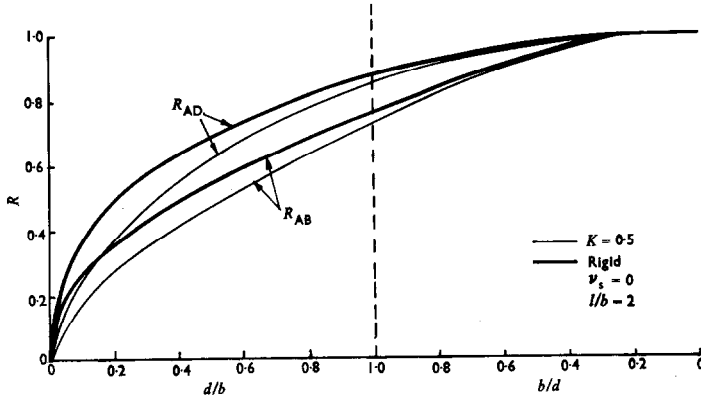
From Fig. 6(b), the correction factor  $R$  for the effect of the finite layer thickness is 1.00. Eqn. (5) then gives

$$m = 1.00 \times 0.05$$

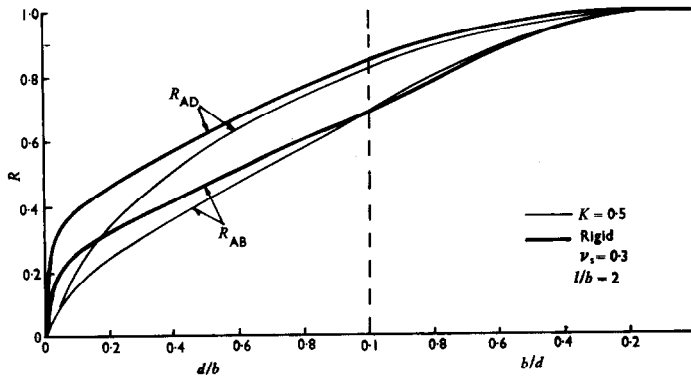
$$= 0.05 \text{ MN m/m}$$

## RESULTS FOR MULTI-LAYERED SYSTEMS

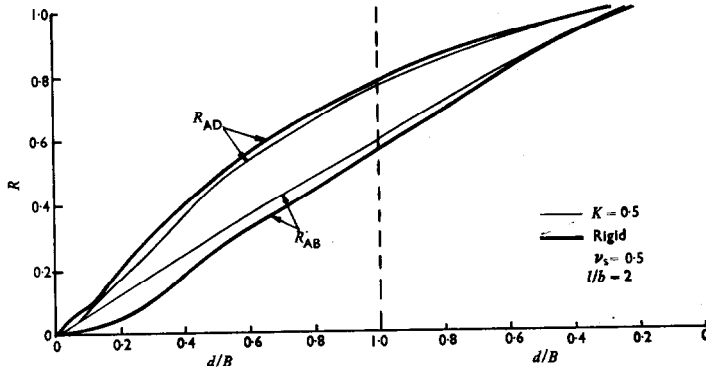
Although the computer model program FOCALS can explicitly consider multi-layered systems, an approximate graphical design method is needed for many routine design problems. By weighting the elastic parameters of each layer in a multi-layered system according to its influence on settlement an 'equivalent' modulus and Poisson's ratio can be determined for



(a)



(b)



(c)

Fig. 10. Bending moment correction factor  $R(l/b=2)$ : (a)  $\nu_s=0$ ; (b)  $\nu_s=0.3$ ; (c)  $\nu_s=0.5$

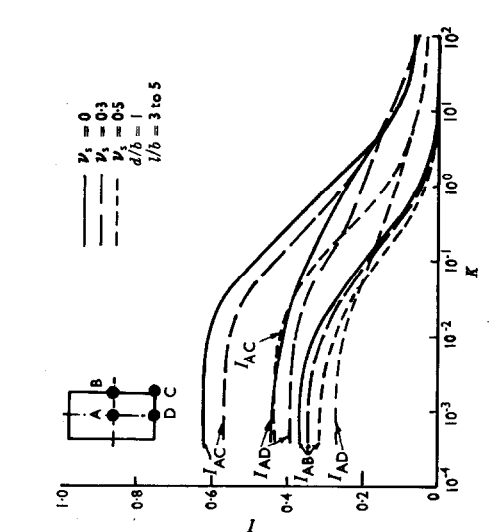
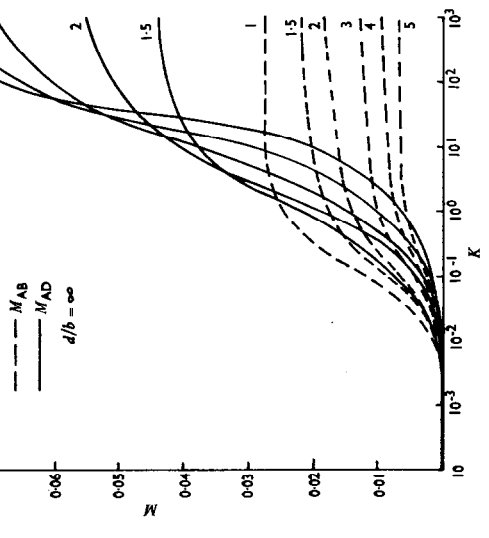
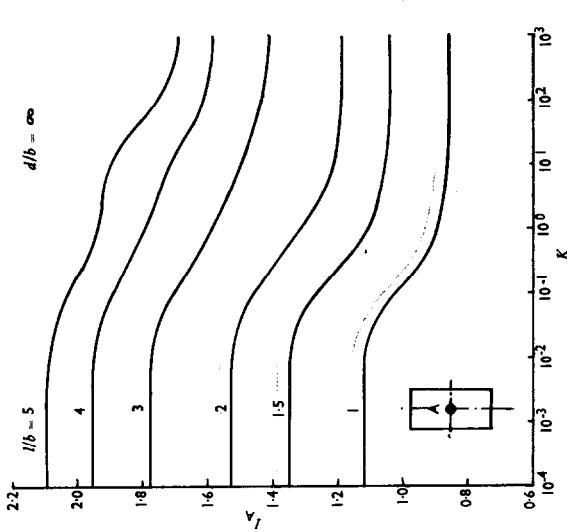
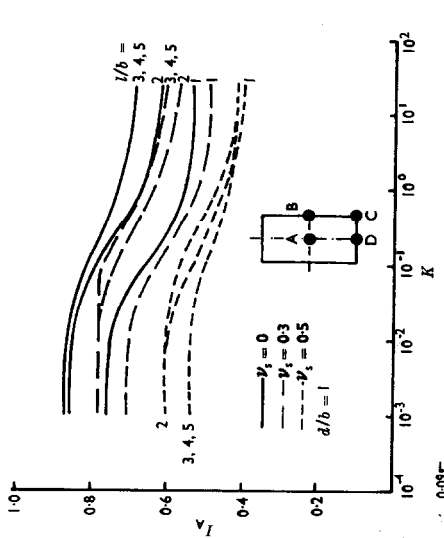
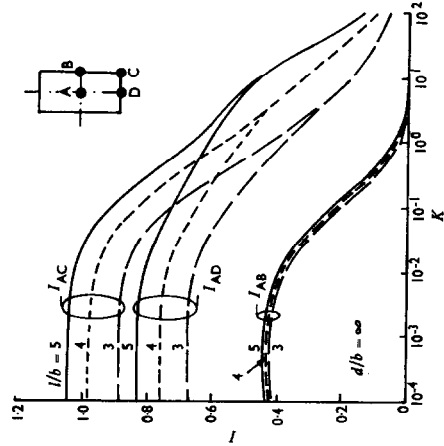


Fig. 11 (above left). Settlement influence factor  $I_A$  for  $d/b = \infty$ , ( $l/b \leq 5$ )  
Fig. 12 (above centre). Settlement influence factor  $I_A$  for  $d/b = 1$ , ( $l/b \leq 5$ )  
Fig. 13 (above right). Differential settlement influence factors  $I_{AB}$ ,  $I_{AC}$ ,  $I_{AD}$  for  $d/b = \infty$ , ( $3 < l/b < 5$ )  
Fig. 14 (far left). Differential settlement influence factors  $I_{AB}$ ,  $I_{AC}$ ,  $I_{AD}$  for  $d/b = 1$ , ( $3 < l/b < 5$ )  
Fig. 15 (left). Bending moment influence factor  $M$  for  $d/b = \infty$ , ( $l/b \leq 5$ )

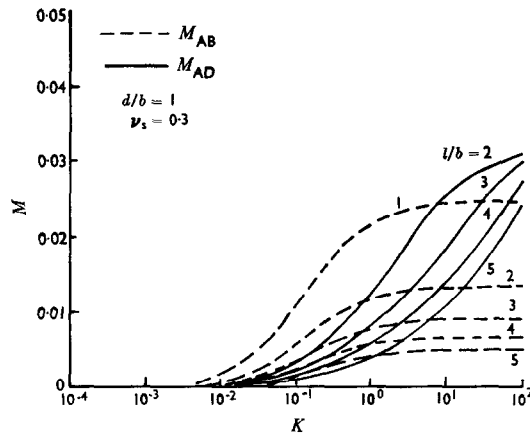


Fig. 16. Bending moment influence factor  $M$  for  $d/b = 1$ ,  $(l/b \leq 5)$

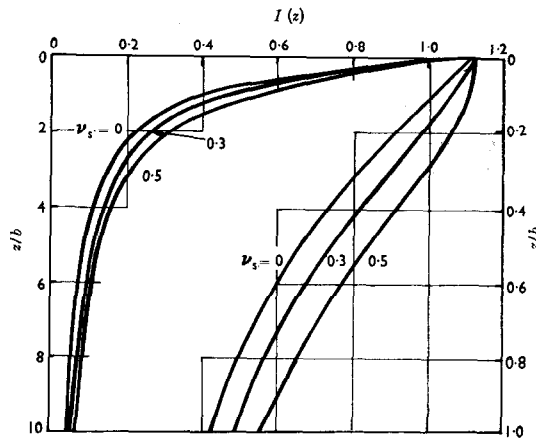


Fig. 17. Vertical settlement influence factor

the overall system. The equivalent elastic parameters can then be used to obtain solutions from eqns (2) and (3).

The approximate equivalent elastic parameters can be obtained as follows. The vertical settlement at depth  $z$  below the centre of a uniformly loaded square flexible raft is given by Harr (1966)

$$\rho(z) = pb \frac{(1-\nu^2)}{E} I(z) \quad \dots \dots \dots (6)$$

where  $I(z)$  is plotted in Fig. 17.

By assuming that the vertical deformation of a layer  $i$  in an  $n$ -layered system is approximately equal to the deformation of that layer in a system where all layers have been replaced by material from layer  $i$ , the settlement contribution of that layer can be approximated using eqn (6). Summing these contributions for  $n$  layers the total settlement can be equated to the settlement for an equivalent single homogeneous layer, and the equivalent modulus  $\bar{E}$  and equivalent Poisson's ratio are given by

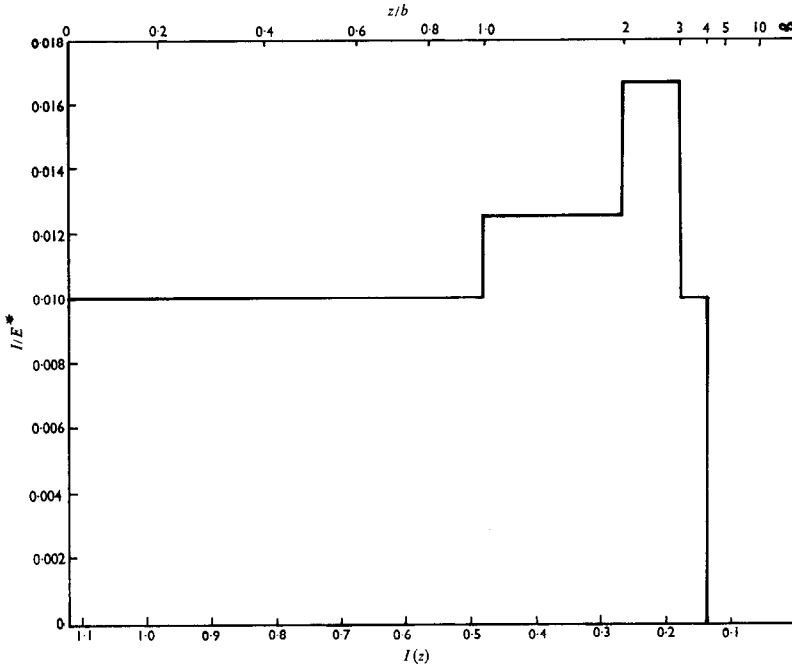


Fig. 18. Variation of  $1/E^*$  with depth  $z/b$

$$\frac{1}{\bar{E}^*} = \sum_{i=1}^n \frac{1}{E_i^*} \Delta I^i / \Delta I^{\text{total}} \quad . \quad . \quad . \quad . \quad . \quad . \quad (7a)$$

and

$$\bar{\nu} = \sum_{i=1}^n \nu_i \Delta I^i / \Delta I^{\text{total}} \quad . \quad . \quad . \quad . \quad . \quad . \quad (7b)$$

where  $E^* = E/(1 - \nu^2)$ .

$E_i^*$ ,  $\nu_i$  are the elastic parameters for layer number  $i$  in the  $n$ -layered system, and  $\Delta I^i = I(z_{\text{top}}^i) - I(z_{\text{bottom}}^i)$  where  $z_{\text{top}}^i$ ,  $z_{\text{bottom}}^i$  are the depths below the surface of the top and bottom of layer number  $i$ , and  $\Delta I^{\text{total}} = I(0) - I(d)$  where  $d$  is the depth of the base of the bottom layer.

The task of determining the equivalent modulus is simplified by plotting values of  $1/E_i^*$  using a horizontal scale which is linear with respect to  $I(z)$ , but for convenience is labelled with values of  $z/b$  (see Fig. 18). The value of  $1/\bar{E}^*$  is then simply the 'average' value of  $1/E^*$ , weighted according to the special horizontal scale.

For a system with unequal Poisson's ratios,  $\bar{\nu}$  can be obtained by plotting  $\nu$  against  $z/b$  using the special scale provided in Fig. 18.

For a system with all Poisson's ratios equal,  $\bar{\nu} = \nu_i$  and eqn (7a) becomes

$$\frac{1}{\bar{E}} = \sum_{i=1}^n \frac{1}{E_i} \Delta I^i / \Delta I^{\text{total}} \quad . \quad . \quad . \quad . \quad . \quad . \quad (8)$$

An example that demonstrates the approximate method follows; the example consists of a square raft and four different soil layers resting on a rigid base (Fig. 19). The variation of  $1/E^*$  is plotted against the special  $z/b$  scale as shown on Fig. 18. Summing the areas under the curve gives

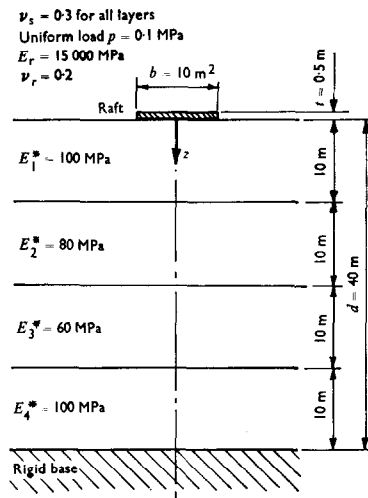


Fig. 19. Details of example

$$\text{Area} = \frac{1.12 - 0.48}{100.0} + \frac{0.48 - 0.26}{80.0} + \frac{0.26 - 0.18}{60.0} + \frac{0.18 - 0.14}{100.00} = 0.01088$$

Giving

$$\begin{aligned} \bar{E}_s^* &= \frac{1.12 - 0.14}{0.01088} \\ &= 90.0 \text{ MPa} \end{aligned}$$

and since  $\nu$  of each of the layers equals 0.3,  $\bar{\nu} = 0.3$  giving  $\bar{E}_s = 81.9$  MPa.

The approximate settlements and maximum bending moment for the multi-layered medium are obtained by considering a homogeneous layer with the 'equivalent' elastic parameters  $E_s = 81.9$  MPa and  $\nu_s = 0.3$ . The same rigid base depth ( $d/b = 4.0$ ) is used for both the actual medium and the 'equivalent' medium. The results for the settlements and maximum bending moment of the equivalent medium (these were determined in the numerical example presented earlier) are given below. The quantities in brackets are the exact results obtained from the computer model.

Central settlement,  $\rho_A = 0.0107$  m (0.0114 m)

Differential settlement,  $\rho_{AB} = 0.0029$  m (0.0027 m)

Maximum bending moment,  $m = 0.050$  MN m/m (0.044 MN m/m)

## CONCLUSIONS

Graphical solutions for settlements, differential settlements and maximum bending moment for uniformly loaded rectangular rafts of arbitrary rigidity have been presented.

The relative stiffness factor  $K$  of the raft-soil system is a major factor in determining its performance.

The detailed variation of soil properties with depth must be taken into account in a rational raft design. For example, for a square raft on a layer thickness equal to the raft width, predictions of total settlement differ by as much as 55%, differential settlement by 18% and maximum bending moment by 15%, when compared with solutions for a semi-infinite soil.



By weighting the elastic parameters of a multi-layered soil system according to their approximate contribution to vertical settlement, an approximate 'equivalent' modulus can be obtained. Hence the solutions for a single soil layer can be used for multi-layer systems.

The solutions for uniformly loaded rafts presented should be adequate for preliminary design purposes. However, for a complete analysis, taking into account actual column loads and superstructure rigidity, a computer program such as FOCALS must be used.

# ACKNOWLEDGEMENT

Thanks are due to Mr G. Bonner for assistance with the computational work.

# APPENDIX: CROSS-ANISOTROPIC SEMI-INFINITE MEDIUM

The results presented for the isotropic semi-infinite medium can also be applied to a cross-anisotropic semi-infinite medium. The stress-strain relationships for a cross-anisotropic material whose axis of elastic symmetry (z) is vertical can be written

$$\left. \begin{aligned} \epsilon_x &= \frac{\sigma_x}{E_h} - \nu_h \frac{\sigma_y}{E_h} - \nu_{vh} \frac{\sigma_z}{E_v} \\ \epsilon_y &= -\nu_h \frac{\sigma_x}{E_h} + \frac{\sigma_y}{E_h} - \nu_{vh} \frac{\sigma_z}{E_v} \\ \epsilon_z &= -\nu_{hv} \frac{\sigma_x}{E_h} - \nu_{hv} \frac{\sigma_y}{E_h} + \frac{\sigma_z}{E_v} \\ \gamma_{xy} &= (1 + \nu_h) \frac{\tau_{xy}}{E_h} \\ \gamma_{xz} &= \frac{\tau_{xz}}{f} \\ \gamma_{yz} &= \frac{\tau_{yz}}{f} \end{aligned} \right\} \dots \dots \dots (9)$$

The two Poisson's ratios  $\nu_{hv}$  and  $\nu_{vh}$  are related by

$$\nu_{vh}/E_v = \nu_{hv}/E_h \dots \dots \dots (10)$$

The vertical settlement  $\rho(r)$  at the surface of a cross-anisotropic semi-infinite medium loaded by a concentrated vertical force  $P$  is given by Gerrard and Wardle (1973) as

$$\rho(r) = \frac{\alpha(a_{11}a_{33})^{1/2}}{a_{11}a_{33} - a_{13}^2} \frac{P}{\pi r} \dots \dots \dots (11)$$

where  $r$  is the distance from the load to the point of interest, and

$$\left. \begin{aligned} a_{11} &= E_h(1 - \nu_{hv}\nu_{vh})(1 + \nu_h)^{-1}(1 - \nu_h - 2\nu_{hv}\nu_{vh})^{-1} \\ a_{33} &= E_h\nu_{vh}(1 - \nu_h - 2\nu_{hv}\nu_{vh})^{-1} \\ a_{13} &= E_v(1 - \nu_h)(1 - \nu_h - 2\nu_{hv}\nu_{vh})^{-1} \\ \alpha^2 &= [a_{11}a_{33} - a_{13}^2 + f(a_{11}a_{33})^{1/2}](2a_{33}f)^{-1} \end{aligned} \right\} \dots \dots \dots (12)$$

For an isotropic semi-infinite medium, eqn (11) becomes

$$\rho(r) = \frac{E_s}{1 - \nu_s^2} \frac{P}{\pi r} \dots \dots \dots (13)$$

Comparison of eqns (11) and (13) shows that the vertical load/surface vertical settlement response of a given cross-anisotropic semi-infinite medium will be the same as that of an isotropic medium for which

$$\frac{E_s}{1 - \nu_s^2} = \frac{\alpha(a_{11}a_{33})^{1/2}}{a_{11}a_{33} - a_{13}^2} \dots \dots \dots (14)$$

Using eqn (14), the results for the isotropic semi-infinite medium can be applied to cross-anisotropic semi-infinite media. Note that only the constant  $E_s/(1 - \nu_s^2)$  needs to be determined; actual values of  $E_s$  and  $\nu_s$  are not required.

## REFERENCES

- Absi, E. (1970). Étude de problèmes particuliers. *Annls Inst. Tech. Bâtim.*, No. 265, 173–188.
- Brown, P. T. (1972). *Analysis of rafts on clay*. PhD thesis, University of Sydney, Australia.
- Butterfield, R. & Banerjee, P. K. (1971). A rigid disc embedded in an elastic half space. *Geotech. Engng* 2, No. 1, 35–52.
- Chan, H. C. & Cheung, Y. K. (1974). Contact pressure of rigid footings on elastic foundations. *Civ. Engng*, April, 51–59.
- Cheung, Y. K. & Zienkiewicz, O. C. (1965). Plates and tanks on elastic foundations—an application of finite element method. *Int. Jnl Solids Structures* 1, No. 4, 451–461.
- Cheung, Y. K. & Nag, D. K. (1968). Plates and beams on elastic foundations—linear and non-linear behaviour. *Géotechnique* 18, No. 2, 250–260.
- Gerrard, C. M., Davis, E. H. & Wardle, L. J. (1972). Estimation of the settlements of cross-anisotropic deposits using isotropic theory. *Aust. Geomech. Jnl* G2, No. 1, 1–10.
- Gerrard, C. M. & Harrison, W. J. (1971). *The analysis of a loaded half-space comprised of anisotropic layers*. Technical Paper No. 10. Melbourne: CSIRO Division of Applied Geomechanics.
- Gerrard, C. M. & Wardle, L. J. (1973). *Solutions for point loads and generalized circular loads applied to a cross-anisotropic half-space*. Technical Paper No. 13. Melbourne: CSIRO Division of Applied Geomechanics.
- Giroud, J. P. (1972). Settlement of rectangular foundation on soil layer. *Jnl Soil Mech. Fdn Div. Am. Soc. Civ. Engrs* 98, SM1, 149–154.
- Gorbunov-Possadov, M. I. & Serebrjanyi, R. V. (1961). Design of structures on elastic foundations. *Proc. Fifth Int. Conf. Soil Mech. Fdn Engng, Paris* 1, 643–648.
- Harr, M. E. (1966). *Foundations of theoretical soil mechanics*. New York: McGraw-Hill.
- Hooper, J. A. (1974). Analysis of a circular raft in adhesive contact with a thick elastic layer. *Géotechnique* 24, No. 4, 561–580.
- Hooper, J. A. (1975). Elastic settlement of a circular raft in adhesive contact with a transversely isotropic medium. *Géotechnique* 25, No. 4, 691–711.
- Milovic, D. M. & Tournier, J. P. (1971). Stresses and displacements due to rectangular load on a layer of finite thickness. *Soils Fdns* 11, No. 1, 1–27.
- Svec, O. J. & Gladwell, G. M. L. (1973). A triangular plate bending element for contact problems. *Int. Jnl Solids Structures* 9, 433–446.
- Ueshita, K. & Meyerhof, G. G. (1968). Surface displacements of an elastic layer under uniformly distributed loads. *Highw. Res. Record*, No. 288, 1–10.
- Wardle, L. J. & Fraser, R. A. (1974). Finite element analysis of a plate on a layered cross-anisotropic foundation. *Proc. First Int. Conf. Finite Element Methods Engng, University of NSW*, 565–578.
- Wardle, L. J. & Fraser, R. A. (1975). *Program FOCALS—foundation on cross anisotropic layered system—user's manual*. Geomechanics Computer Program No. 4. Melbourne: CSIRO Division of Applied Geomechanics.